sciendo   RIGA TECHNICAL UNIVERSITY

A New RMF Stirrer Using AISI4140 Mild Steel: Energy Optimization Application

Hakan Citak* (*Assoc. Professor, Balikesir University, Balikesir, Turkey*),
Sabri Bicakci (*Assoc. Professor, Balikesir University, Balikesir, Turkey*),
Mustafa Coramik (*Assoc. Professor, Balikesir University, Balikesir, Turkey*),
Huseyin Gunes (*Assoc. Professor, Balikesir University, Balikesir, Turkey*),
Yavuz Ege (*Professor, Balikesir University, Balikesir, Turkey*)

Abstract – **This study examines the development of a novel FPGA-based RMF stirrer system. The system has been designed as a 3-phase system, with each phase being fed by PWM voltage with a phase difference of 120°. In case the system is driven at a 100 % duty cycle, the force acting on the magnetic fish remains continuous and constant until the subsequent phase changes. In such a case, at speeds under 400 rpm, the speed of the magnetic fish fails to be synchronized with the phase change speed. The magnetic fish, therefore, rotates more than 120° and the force is observed to cause a braking effect. Both fluid logic control (FLC) and virtual model control (VMC) were utilised to enable the system to be driven at a different duty cycle. The energy efficiency of the system for fluids with different viscosities has been attempted to be thereby improved with a lower current and shorter excitation time. With FLC and VMC control, the energy consumed by the system is reduced and the efficiency is increased, and approximately 95 % energy gain is obtained for liquids with viscosity up to 1.03 Pa·s. It has been experimentally proven that a lower limit value of the duty cycle of the PWM signal applied to the drive circuit of the system depends on the viscosity of the mixed liquid and a lower limit value increases with increasing viscosity. It has also been found that controlling the system with FLC and VMC does not have a great effect on the energy gain.**

Keywords – **Efficiency, FPGA, fuzzy logic control, PWM modulation, RMF stirrer, virtual model control.**

I. INTRODUCTION

First patented by Arthur Rosinger in 1944, operating principles of electromagnetic stirrers have undergone changes in time [1]. Early on, magnet pairs fixed on the rotor of a conventional electric motor were used for stirring different fluid products. Being referred to as motor stirrers, such electromagnetic stirrers utilise rod magnets for stirring, which follow the rotation of the magnet pair fixed on the rotor of the motor and stir the fluid they are in [2]–[4]. However, particularly at low speeds, the magnet inside the fluid deviates from the centre of rotation and sticks to one of the pair of magnets which provide rotation. This results in the termination of the stirring process. Furthermore, additional connections, which connect the rotor of the electric motor to the magnet pair, cause a certain part of the energy transferred to the rotor to be lost. This reduces the efficiency of the system. Therefore, RMF stirrers are now used for the stirring process [5]–[9]. RMF stirrers are actually axial flux synchronous motors [10]–[17]. The difference of such stirrers from others is the absence of a physical connection between the magnetic fish acting as the rotor and the source of the magnetic field. The magnetic fish follows the rotation of the magnetic field. The rotating magnetic field generated by such stirrers also allows direct stirring of liquid metals [18]. The literature contains studies incorporating magneto-hydrodynamic (MHD) stirrers, where a rotational magnetic field (RMF) and traveling magnetic field (TMF) are used in combination [19]–[22]. MHD stirrers not only ensure toroidal flow in the solution with RMF, but also poloidal flow utilising TMF. Therefore, MHD stirrers incorporate two independent coil systems [23], [24].

The deposit, which accumulates on the surface of the fluid due to the centrifugal force resulting from the rotating movement of the RMF, is pushed downward by the TMF. The downward force generated by the TMF creates a downward flow near the wall. Said downward flow impacts the bottom surface and changes direction, creating an upward flow at the centre, which pushes up the lower part of the fluid level deformation. Consequently, fluid surface deformation is reduced. As RMF and TMF can be controlled independently, the fluid level can be kept constant by adjusting the TMF current according to the deformation of the fluid level [25]. As MHD stirrers allow for creation of various hydrodynamic structures and flexible control of their behaviour, they are widely used in many areas of science and technology [26]. However, RMF stirrers are preferred more since they can be used even for fluids with low electrical conductivity, such as aqueous solutions. In the literature, such stirrers are mostly utilised in fluid flow and crystal growth applications [27]. RMF stirrer is preferred in this study because of its wide range of applications. The literature demonstrates that RMF stirrers are generally produced as 3-phase systems, where a rotational magnetic field is generated by applying different voltages to each phase [28]. It is further seen that amplitudes of the square wave voltages are not changed albeit the phases are different,

---

* Corresponding author. E-mail: hcitak@balikesir.edu.tr

and, therefore, the magnetic fish is exposed to a constant magnetic force. This results in constant acceleration and a speed, which constantly increases until the change of the phase. In such a case, especially at speeds under 400 rpm, the speed of the magnetic fish fails to be synchronized with the phase change speed. The magnetic fish, therefore, rotates more than the phase angle and the force is observed to cause a braking effect, with the fish rotating back at an angle equal to that it has swept in excess. The angle swept in excess is dependent on the viscosity of the stirred fluid. The lack of synchronization between the speed of the magnetic fish and the phase change speed reduces the system's energy efficiency. In this study, different from our other study, a new RMF stirrer system was developed. In this new stirrer, magnetic core (AISI4140), application voltage (16 V) was changed and a new control program (VMC) was developed. By increasing the magnetic permeability of the magnetic core and the application voltage, it was aimed to increase the rotating magnetic field and the force acting on the magnetic fish. Thus, it was ensured that liquids with different viscosities could be mixed. By using both FLC and VMC control methods for each liquid, it was ensured that the system was driven with different duty cycles without losing the speed of the magnetic fish. Thus, the energy gain of the system was tried to be increased with a lower current and lower excitation time. The relationship between the viscosity of the mixed liquid and the energy efficiency was tried to be determined by the lower limit value of the duty cycle of the PWM signal applied to the control circuit of the system. This study, which focuses on increasing the energy efficiency of RMF stirrer according to the viscosity of the mixed liquid, differs from the studies in the literature in this respect.

Section II of the paper presents the selection and fabrication of the stirrer core and the winding and electronics of the coil; Sections III and IV present the details of the LabVIEW-based control program of the developed stirrer. Section V presents the experimental findings, and the last section presents the conclusions and recommendations.

II. MATERIAL AND METHOD

The study began with research for a core steel for the RMF stirrer, and the American Iron and Steel Institute's AISI4140 mild steel was preferred due to its low H_c critical value. The mild steel was machined into a cylindrical disc with a diameter of 130 mm and a height of 35 mm. The production of the 12-section core was completed by opening 5 mm wide and 25 mm deep canals (teeth) on the upper surface of the disc. The core was left under magnetic field for a day in order to remove the stress resulting from the machining process and was further rested for a certain period of time prior to winding. Chemical components of the mild steel used for core production are provided in Table I. In the next step, windings for the 3 phases were made on the core of the RMF Stirrer, as shown in Fig. 1. Each phase comprised of 150 windings using copper wire with a diameter of 0.5 mm.

TABLE I

CHEMICAL COMPOSITION OF THE AISI4140 MILD STEEL IN TERMS OF % WEIGHT

Material	C	Si	Mn	P	S	Cr	Mo	Ni
AISI 4140	0.45	0.40	0.90	0.025	0.035	1.20	0.30	0.40

(a)	(b)	(c)
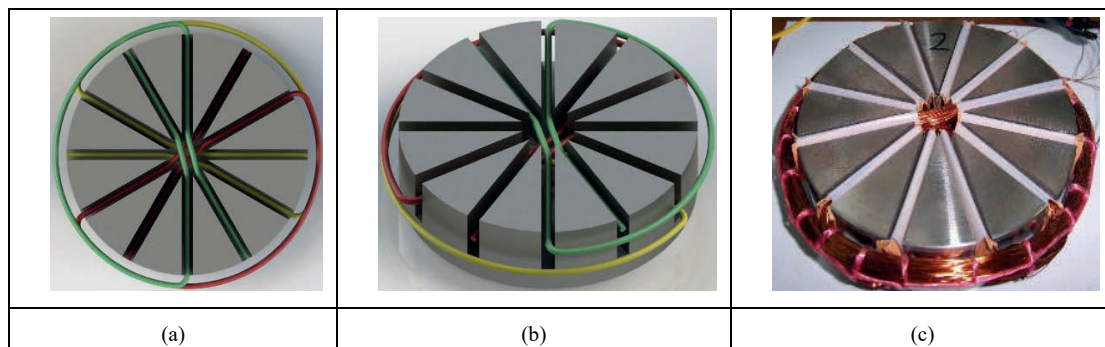
Fig. 1. a); b) Core and winding design of the RMF Stirrer; c) final product.

Development of the RMF stirrer stator (core) was followed by the design of the electronic driver circuit capable of applying PWM voltage to the windings for the R, S and T phases with a phase difference of 120 degrees (Fig. 2a). The windings were fed using an L298N step motor driver IC. 3 L298N ICs were actively operated for the windings of each coil. This enabled a current up to 3A to flow through each stator coil. The current flow was measured using an ACS714 current sensor. In addition, a UGN3177UA Hall effect sensor was used for contact-free measurement of the rotational speed of the magnetic fish. The sensor was fixed on a plexiglass plate and positioned between the beaker and the RMF stirrer core (Fig. 2b). The sensor generated one square wave per one full rotation of the magnetic fish inside the beaker (Fig. 2c).
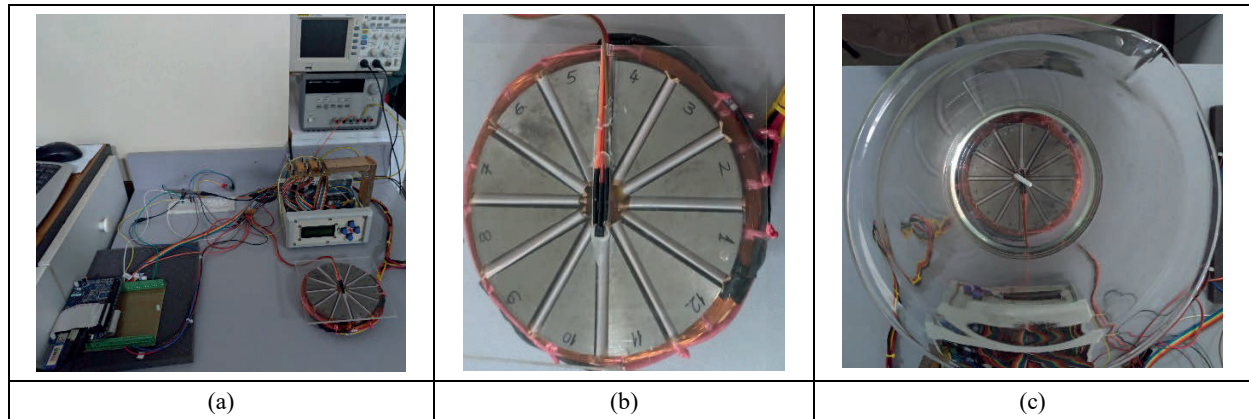
Fig. 2. a) Electronic component box of the developed RMF Stirrer; b) UGN3177UA Hall effect sensor location; c) Rotational centre of the magnetic fish.

The FPGA structure within the NI myRIO 1950 embedded system was utilised in the study for sequential control of the phases, generation of the PWM signal and determination of the increment range of the phase frequency and the rotational speed of the magnetic fish. The ARM microcontroller structure of the myRIO embedded system was utilised in the RMF stirrer system to adjust the duty cycle values of the FLC and VMC voltages. LabVIEW software interface was used to program the myRIO embedded system.

A total of eight fluids with different viscosities, which are frequently used in scientific laboratories, were used in the study. Technical characteristics of such fluids are provided in Table II, and photographs thereof are demonstrated in Fig. 3.

TABLE II
TECHNICAL CHARACTERISTICS OF THE FLUIDS USED FOR TESTING

Name	Formula	Viscosity (Pa·s)	Density (g/cm³)
Water	H_2O	0.001	1
Ethylene Glycol	$C_2H_6O_2$	0.0161	1.11
Dioctyl Adipate	$C_{22}H_{42}O_4$	0.019	0.926
Polyethylene Glycol (PEG 400)	$C_{16}H_{34}O_9$	0.12	1.126
Sodium Silicate Module 3	Na_2SiO_3	0.15	2.4
Engine Oil SAE 10W/40	ASTM D445	1.03	0.87702
Engine Oil SAE 20W/50	ASTM D445	1.35	0.90864
Glycerin	$C_3H_8O_3$	1.48	1.26
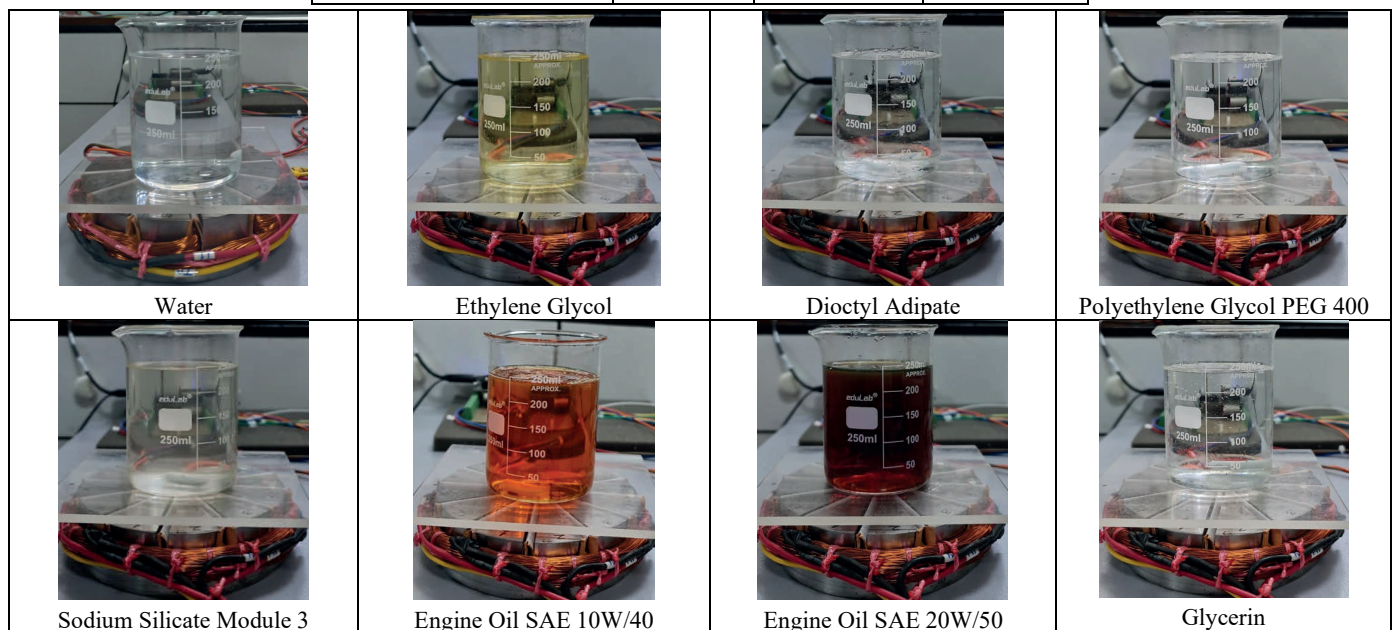
Fig. 3. Photographs of the test fluids.

III. Developed LabVIEW Software for RMF Stirrer

Programming of the myRIO 1950 embedded system, which is used to control the duty cycle of the PWM signal applied to the RMF stirrer, was conducted using the graphical interface of the LabVIEW software. The user interface of the software allows for the input of the target speed of the magnetic fish and the other control conditions, which can also be changed, while the program is in operation. Sending of driver signals based on control conditions and the evaluation of the sensor signals are carried out on the FLC and VMC myRIO platforms. The PC is used solely to display the results.

The FPGA system on the myRIO platform incorporates four circuits, which run in parallel. The first circuit reads the period of the square wave generated by the hall sensor, through which the rotational speed of the fish is determined. The second circuit reads the analogue signal received from the current sensor as raw data, which enables the calculation of the current drawn by the RMF stirrer.

The third circuit enables rotating of the magnetic fish at a speed ranging from an initial value of 300 rpm to the reference speed entered into the interface, with acceleration in the desired steps. The circuit calculates the required triggering time-based on instantaneous speed and sequentially changes the logic states of the R, S and T phases.

The final circuit generates the PWM signal based on the PWM frequency entered via the interface. The duty cycle value of the PWM signal is the output value of the FLC or VMC controller, which runs on the ARM Cortex A9 microprocessor in the myRIO platform. Whereas on the ARM Cortex A9 microcontroller on the myRIO platform, the designed FLC or VMC controller runs at the cycle speed entered via the interface, the required control commands are sent to the FPGA circuits and data received from the FPGA are read, processed and sent to the interface screen. Furthermore, a step reference generator was programmed in order to enable testing of the system. Figure 4a exhibits the LabVIEW block diagram for the microcontroller program. Figure 4b exhibits the Front Panel of the developed LabVIEW software.
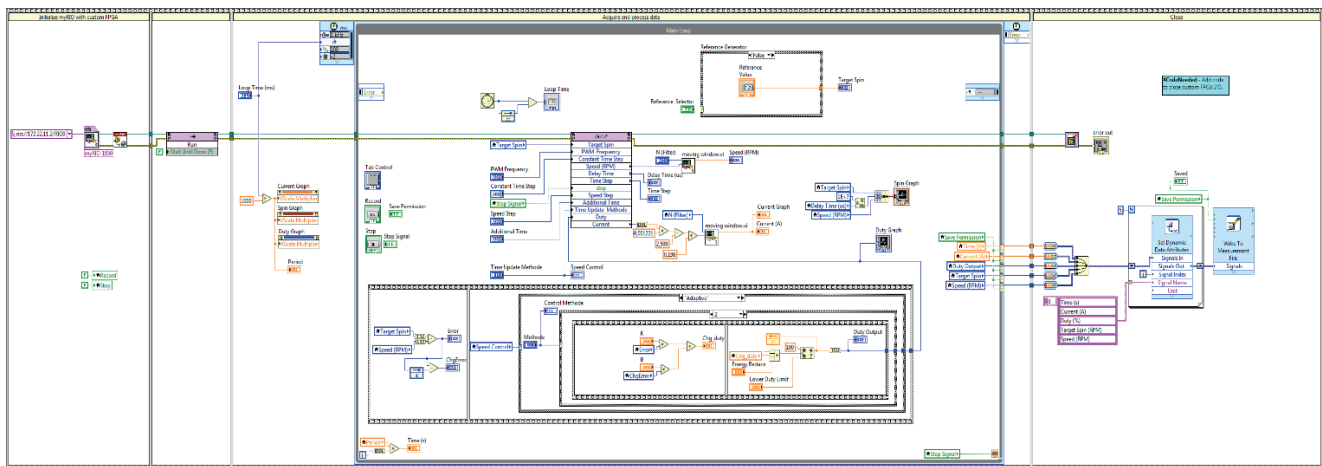
(a)

(b)

Fig. 4. a) LabVIEW Front Panel; b) LabVIEW block diagram of the microprocessor program.

IV. FUZZY LOGIC AND VIRTUAL MODEL CONTROLLER

A. *Fuzzy Logic Control (FLC)*

The duty cycle value of the PWM signal, which is applied to the input of the L298N IC in the driver circuit to allow cutting of driver signals at high frequency, is updated via the Takagi-Sugeno Type Zero fuzzy controller. The duty cycle value at the output of the fuzzy controller is continuously reduced by a user-adjustable constant in order both to minimize the error between the fan speed and the rotational speed of the fish and to reduce energy consumption.

FLC inputs are set as the speed error of the magnetic fish and the change of such an error. FLC output is the change value of the cycle to be applied to the driver IC. The duty cycle value is calculated using the formula specified in (1).

$$\%D_{\text{new}} = \%D + \%\dot{D} + \%R_D, \qquad (1)$$

where $\%D_{new}$ is the new duty cycle value, $\%D$ is the old duty cycle value, $\%\dot{D}$ is the output of the FLC, $\%R_D$ is the energy reduction step constant. Seven triangular membership functions (Negative Big – NB, Negative Medium – NM, Negative Small – NS, Zero – Z, Positive Small – PS, Positive Medium – PM, and Positive Big – PB) were selected for the FLC input variables, values of which are provided in Table III. The 49-entry rule bases are provided in Table IV.

TABLE III
THE VALUES OF THE MEMBERSHIP FUNCTIONS OF THE OUTPUT, %*D*

Membership functions	Output value
NB	−5
NM	−3
NS	−1
Z	0
PS	1
PM	3
PB	5

TABLE IV
THE RULE BASES OF THE FLC

		Membership function of the $\dot{e}_w$						
		NB	NM	NS	Z	PS	PM	PB
Membership function of the e_w	NB	NB	NB	NB	NB	NM	NS	Z
	NM	NB	NB	NB	NM	NS	Z	PS
	NS	NB	NB	NM	NS	Z	PS	PM
	Z	NB	NM	NS	Z	PS	PM	PB
	PS	NM	NS	Z	PS	PM	PB	PB
	PM	NS	Z	PS	PM	PB	PB	PB
	PB	Z	PS	PM	PB	PB	PB	PB

The output value of the FLC is calculated based on the formula (2), using the weighted average value method for all rule outputs.

$$\text{Output} = \frac{\sum_{i=1}^{49} w_i \cdot z_i}{\sum_{i=1}^{49} w_i}, \qquad (2)$$

where w_i is the firing strength of the rules and z_i are the values of the output membership functions.

B. *Virtual Model Control*

Virtual Model Control (VMC) is a method for keeping a control variable in a system at a desired position or value, which utilises the effects of virtual mechanical elements as if they are actually in the system [29]. In this study, the duty cycle value of the RMF stirrer developed using the VMC method was attempted to be reduced without disrupting rotational synchronization, for which the function shown in (3) was utilised.

$$\text{Duty}(k+1) = \text{Duty}(k) + f(e(w)) + C_{\text{energy\_reduce}}, \quad (3)$$

where $C_{\text{energy\_reduce}}$ is the reduction step constant applied to ensure continuous reduction of the duty cycle value. In the study, $C_{\text{energy\_reduce}}$ was determined as −0.1, using the trial-and-error method. In order to eliminate any undesired reduction or exceedance in the speed of the magnetic fish during reduction of the duty cycle, the $f(e(w))$ term was determined using the VMC method. In the application of the said method, the position where the error value $e(w)$ for the speed of the magnetic fish is zero was selected as the resting position. The value of $f(e(w))$ was defined with a virtual spring and damper

pair, which extends or compresses based on changes in the error of speed (Fig. 5). In the study, the $f(e(w))$ term was calculated using (4), with $K = 0.02$ and $B = 0.6$.

$$f(e(w)) = K \cdot e(w) + B \cdot \dot{e}(w). \qquad (4)$$

Definitions of symbols in the equations are given in the nomenclature table in Appendix A.
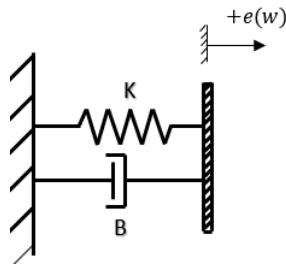
Fig. 5. Virtual spring and damper pair with the resting position where $e(w) = 0$.

V. EXPERIMENTAL FINDINGS

In the experimental phase of the study, lower limit values were determined for the duty cycle where the phase change speed, provided in Table II for fluids with different viscosities, and the rotational speed of the fish are synchronized, and such values are shown in Table V.

TABLE V
DUTY CYCLE LOWER LIMITS AND ENERGY GAINS, DETERMINED USING FLC AT A PHASE VOLTAGE OF 16 V

Name	Formula	Viscosity (Pa.s)	Lower Duty Limit	Energy gain
Water	H_2O	0.001	50 %	96.5 %
Ethylene Glycol	$C_2H_6O_2$	0.0161	60 %	95.8 %
Dioctyl Adipate	$C_{22}H_{42}O_4$	0.019	60 %	95.8 %
Polyethylene Glycol (PEG 400)	$C_{16}H_{34}O_9$	0.12	65 %	95.5 %
Sodium Silicate Module 3	Na_2SiO_3	0.15	65 %	95.5 %
Engine Oil SAE 10W/40	ASTM D445	1.03	70 %	95.2 %
Engine Oil SAE 20W/50	ASTM D445	1.35	80 %	81.2 %
Glycerin	$C_3H_8O_3$	1.48	90 %	50.5 %

The duty cycle value falling below the lower limit results in a reduction in the current applied to the coils, which, in turn, causes a reduction in magnetic field and magnetic force. In such a case, the magnetic fish is overwhelmed by centrifugal force and its rotation at the centre is disrupted, and the rotational speed cannot be determined using the hall sensor.

Figure 6 exhibits the change over time of the measured speed of the magnetic fish, duty cycle and the current drawn from the system as the reference speed for all fluids is periodically increased from 300 rpm to 400 rpm when FLC is active. For all fluids, the speed of the magnetic fish accelerates to the reference speed of 400 rpm in approximately 2.3 s. The developed FL controller sets the duty cycle of the PWM signal applied to the driver circuit to 100 % until the speed reaches the reference value. Once the reference speed is reached, the FL controller reduces the duty cycle back to the lower limit specified in Table V without changing the speed of the magnetic fish. At such point, the current reduces from 1.55 A to 0.41 A for all fluids other than glycerin and 20W50 engine oil. For glycerin and 20W50 engine oil, the current reduces from 1.55 A to 1.15 A and 0.75 A, respectively. For the above

case, the energy gains in the RMF stirrer based on percentage of reduction in the current and duty cycle are provided in Table V.

On the other hand, Fig. 7 exhibits the change over time of the measured speed of the magnetic fish, duty cycle and the current drawn from the system as the reference speed for all fluids is periodically increased from 300 rpm to 400 rpm when VMC is active. The developed VMC controller sets the duty cycle of the PWM signal applied to the driver circuit to 100 % until the speed of the magnetic fish reaches 400 rpm. Once 400 rpm is reached, the VMC controller reduces the duty cycle back to the lower limit specified in Table VI without changing the speed of the magnetic fish. At such point, the current reduces from 1.55 A to 0.41 A for all fluids other than glycerin and 20W50 engine oil. For 20W/50 engine oil, the current reduces from 1.55 A to 0.7 A, while it was observed that the magnetic fish could not rotate in glycerin even at 100 % duty cycle. For the other fluids, the energy gains in the RMF stirrer based on percentage of reduction in the current and duty cycle are provided in Table VI.

Water

Ethylene Glycol

Dioctyl Adipate

Polyethylene Glycol (PEG 400)

Sodium Silicate Module 3

10W 40 Engine Oil

| 20W 50 Engine Oil | Glycerin |
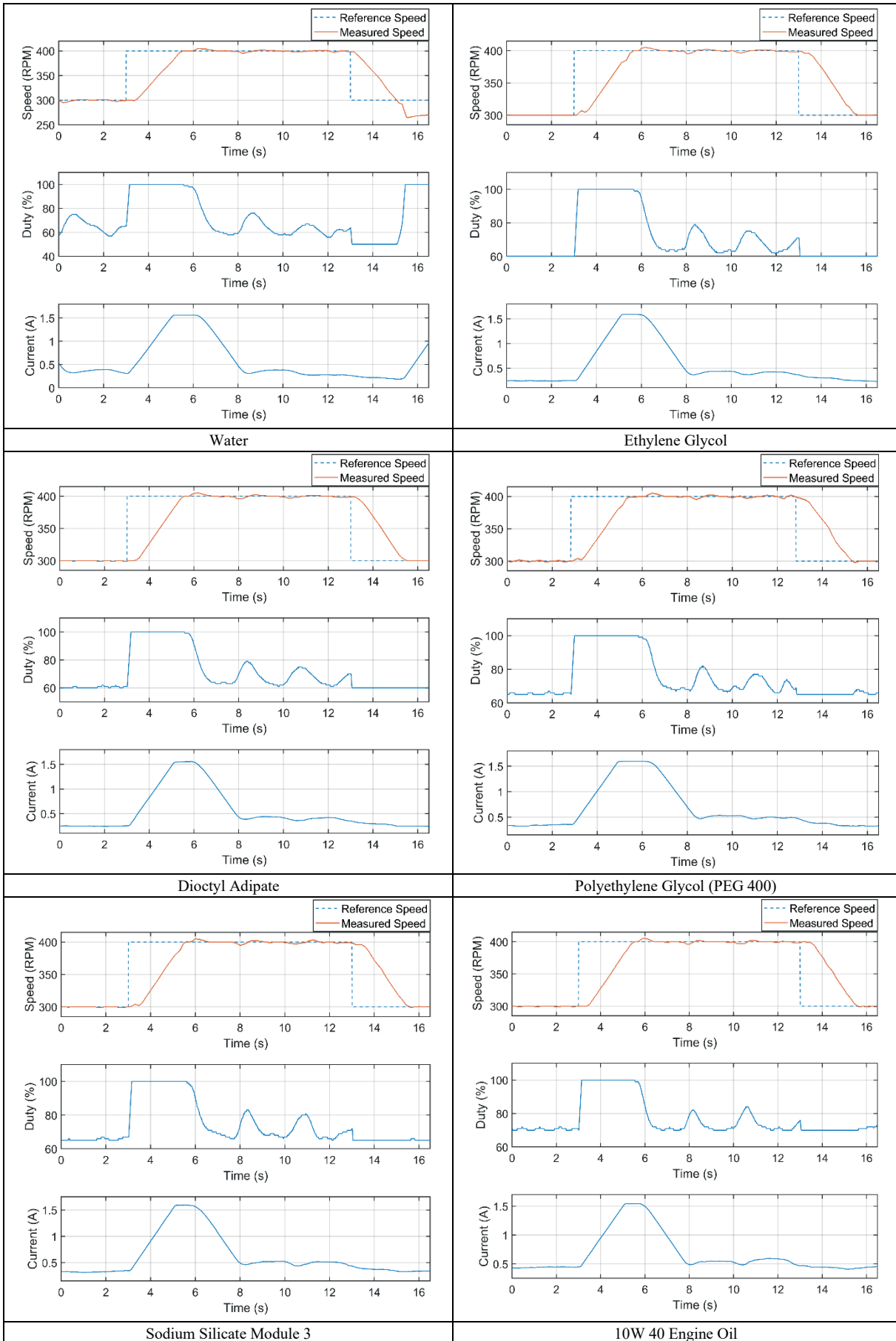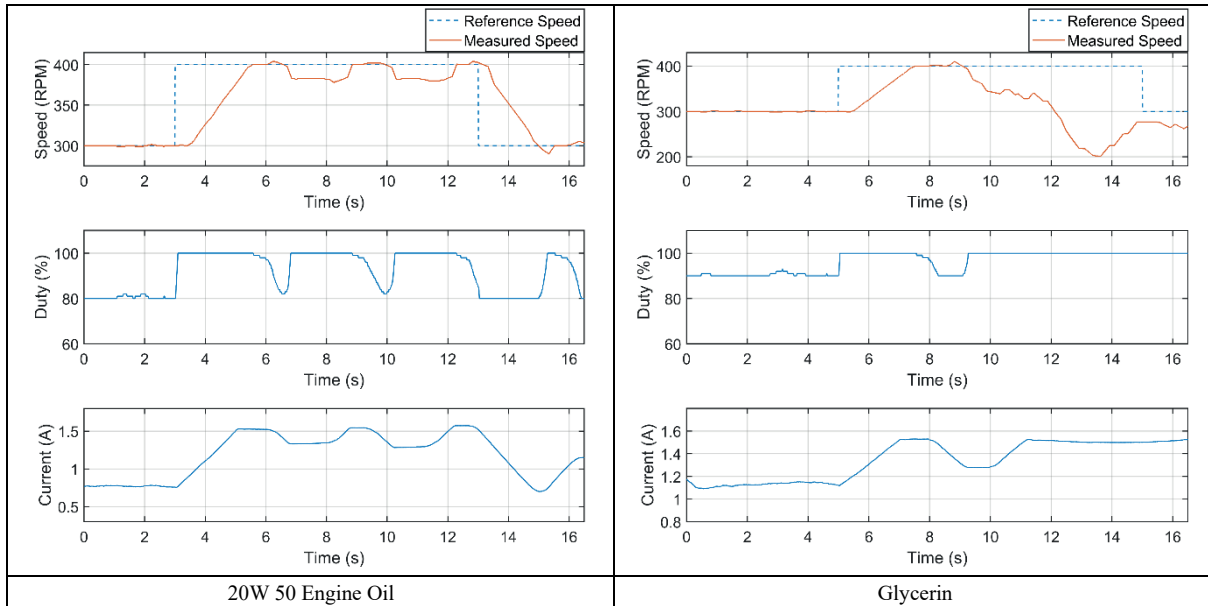
Fig. 6. Change over time of measured speed, duty cycle and current as the reference speed is periodically changed when FLC is active.

TABLE VI

DUTY CYCLE LOWER LIMITS AND ENERGY GAINS, DETERMINED USING VMC AT A PHASE VOLTAGE OF 16 V

Name	Formula	Viscosity (Pa·s)	Lower Duty Limit	Energy gain
Water	H_2O	0.001	55 %	96.2 %
Ethylene Glycol	$C_2H_6O_2$	0.0161	60 %	95.8 %
Dioctyl Adipate	$C_{22}H_{42}O_4$	0.019	60 %	95.8 %
Polyethylene Glycol (PEG 400)	$C_{16}H_{34}O_9$	0.12	65 %	95.5 %
Sodium Silicate Module 3	Na_2SiO_3	0.15	65 %	95.5 %
Engine Oil SAE 10W/40	ASTM D445	1.03	70 %	95.2 %
Engine Oil SAE 20W/50	ASTM D445	1.35	80 %	83.7 %
Glycerin	$C_3H_8O_3$	1.48	No rotation	-

| Water | Ethylene Glycol |
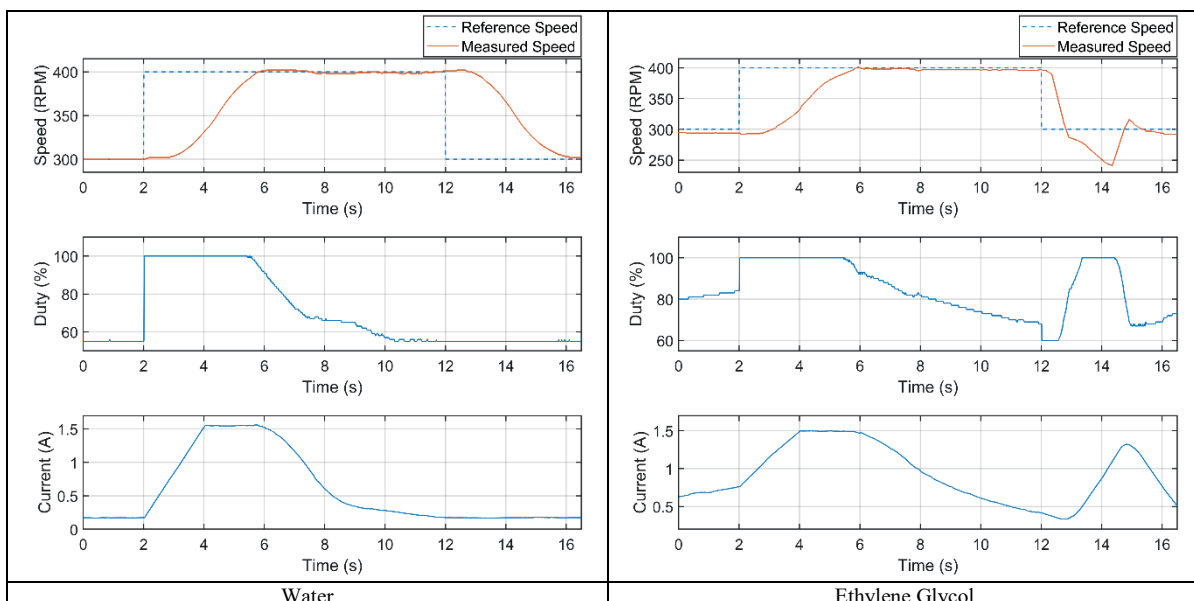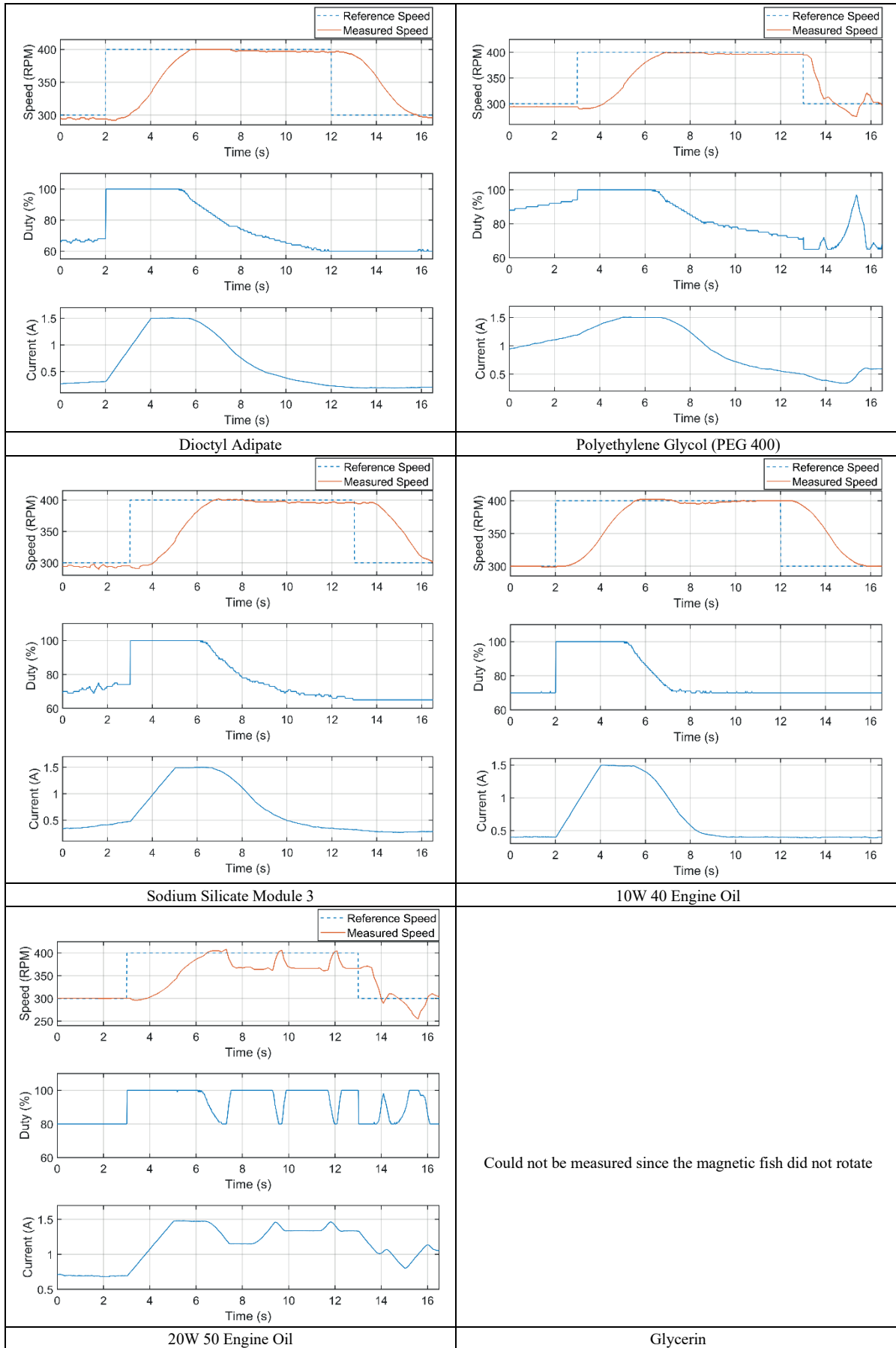
Fig. 7. Change over time of measured speed, duty cycle and current as the reference speed is periodically changed when VMC is active.

VI. Conclusion and Recommendation

This study explored the development of a novel FPGA-based RMF stirrer system. FLC and VMC were utilised to reduce the energy consumption and improve the efficiency of the system, and energy gain percentages were determined for fluids with different viscosities. Reduction in energy consumption was achieved through reduction of the duty cycle of the PWM signal applied to the driver circuit. However, it was experimentally proven for the system in question that the duty cycle lower limit was dependent on the viscosity of the stirred fluid, and the lower limit increased as viscosity increased. This was caused by the fact that the speed gradient of the magnetic fish increased with viscosity, since the synchronization of the speed gradient of the magnetic fish and the phase change speed was not disrupted significantly in a fluid with high viscosity. The excessive rotation of the magnetic fish decreased in each phase, which resulted in the lower limit of the duty cycle to be applied for synchronization to remain high. In addition, it was observed during the experiments that the magnetic fish could not rotate in fluids with high viscosity, such as glycerin, because the magnetic force was too weak. This issue can be resolved by increasing the phase voltage. Moreover, using a stirrer core with greater magnetic permeability or increasing the number of windings may be a solution for increasing magnetic force.

In addition, it was observed that controlling the system with FLC or VMC had no significant impact on the energy gain achieved. This can be explained by the fact that the times required for the calculation and application of the variable values in the control program are similar in both methods. However, in the case of fluids with high viscosity, such as glycerin, the data processing time of the control program would be added to the sequential phase triggering time during the initial start of the rotation of the fish, which is a factor that needs to be taken into consideration in the selection of the control program. In the study, the fact that VMC had a longer data processing time compared to FLC resulted in the fish failing to start rotating in glycerin, and, therefore, no measurements could be taken.

In the literature, there are stirrers with different core and winding structures that perform stirring by creating a rotating magnetic field. In such stirrers, 100 % duty cycle was applied, and the energy spent depending on the frequency was determined as 509 W for 400 rpm [30], [31]. In our study, this value was 24.8 W for 100 % duty cycle and it was reduced by 95 % with duty cycle control.

Although conventional electromagnetic stirrers are widely used in applications in physics, chemistry and biology laboratories, they are not suitable for mixing liquids in closed containers without a specific geometric shape. However, such containers are frequently used in research and quality control laboratories of the pharmaceutical, food, paint and textile industries. In the mixing of liquids with different viscosities in such containers, the importance of stirrers such as the RMF stirrer developed within the scope of the study, which has no rotor and stator connection and can save energy, increases.

Appendix A

Nomenclature

$\%D_{new}$	New duty cycle value
$\%D$	Old duty cycle value
$\%D$	Fuzzy Logic Control output
$\%R_D$	Energy reduction step constant
W_i	The firing strength of the fuzzy rules
Z_i	The values of the output membership function
Duty$(k+1)$	New duty cycle value
Duty(k)	Old duty cycle value
$f(e(w))$	Function of virtual spring and damper pair
$e(w)$	The error of the speed of the magnetic fish
$\dot{e}(w)$	The change in the error of the speed of the magnetic fish
K	Virtual spring constant
B	Virtual damper constant
C_{energy_reduce}	Energy reduction step constant

References

[1] A. Rosinger, "Magnetic stirrer," U.S. Patent 2350534A, June 6, 1944.

[2] K. H. Spitzer, G. Reiter, K. Schwerdtfeger, "Multi-frequency electromagnetic stirring of liquid metals," *ISIJ International*, vol. 36, no. 5, pp. 487–492, 1996. https://doi.org/10.2355/isijinternational.36.487

[3] T. J. Bruno and M. C. Rybowiak, "Vapor entraining magnetic mixer for reaction and equilibrium applications", *Fluid Phase Equilibria*, vol. 178, no. 1–2, pp. 271–276, Mar. 2001. https://doi.org/10.1016/S0378-3812(00)00473-8

[4] F. Barbeu, L. Bahoue, and S. Artemianov, "Energy cascade in a tornado wise flow generated by magnetic stirrer," *Energy Conversion and Management*, vol. 43, no. 3, pp. 399–408, Feb. 2002. https://doi.org/10.1016/S0196-8904(01)00097-8

[5] H. H. Sheu, S. Y. Jian, T. T. Lin, and Y. W. Lee, "Effect of rotational speed of an electromagnetic stirrer on neodymium-doped yttrium aluminium garnet nanoparticle size during co-precipitation," *Microelectronic Engineering*, vol.: 176, pp. 33–39, 2017. https://doi.org/10.1016/j.mee.2017.01.020

[6] M. M. Aboutalebi, F. Lapointe, J. D'amours, M. Isac, and R. I. L. Guthrie, "Numerical modelling of fluid flows in square billet moulds, using a new nozzle orientation in the presence of an in-mould rotary electromagnetic stirrer", *Ironmaking & Steelmaking*, vol. 46, no. 9, pp. 819–826, Aug. 2019. https://doi.org/10.1080/03019233.2018.1510874

[7] Y. Ege, O. Kalender, and S. Nazlibilek, "Electromagnetic stirrer operating in double axis", *IEEE Transactions on Industrial Electronics*, vol. 57, no. 7, pp. 2444–2453, Oct. 2010. https://doi.org/10.1109/TIE.2009.2034676

[8] K. Bolotin, E. L. Shvidkii, I. Sokolov, and S. A. Bychkov, "Shape optimization of soft magnetic composite inserts for electromagnetic stirrer with traveling magnetic field", *Compel – The International Journal for Computation and Mathematics in Electrical and Electronic Engineering*, vol. 39, no. 1, pp. 28–35, Mar. 2020. https://doi.org/10.1108/COMPEL-05-2019-0207

[9] V. I. Milykh and L. V. Shilkova, "Numerical-field calculation of the angle torque characteristic of the three-phase inductor of the magnetic field of the electromagnetic stirrer in processing dissimilar mixtures," *Problemele Energeticu Regionale*, vol. 41, no. 1–2, pp. 55–64, Jun. 2019. https://doi.org/10.5281/zenodo.3239174

[10] S.-H. Park, J.-W. Chin, K.-S. Cha, and M.-S. Lim, "Deep transfer learning-based sizing method of permanent magnet synchronous motors considering axial leakage flux," *IEEE Transactions on Magnetics*, vol. 5, no. 9, Sep. 2022, Art. no. 8206005. https://doi.org/10.1109/TMAG.2022.3181804

[11] K. Yamazaki, K. Utsunomiya, and H. Ohiwa, "Mechanism of torque ripple generation by time and space harmonic magnetic fields in permanent magnet synchronous motors," *IEEE Transactions on Industrial Electronics*, vol. 69, no. 10, pp. 9884–9894, Oct. 2022. https://doi.org/10.1109/TIE.2021.3121713

[12] M. Horiuchi, R. Masuda, Y. Bu, M. Nirei, M. Sato, and T. Mizuno, "Effect of magnetic wedge characteristics on torque ripple and loss in interior permanent magnet synchronous motor," *IEEJ Journal of Industry Applications*, vol. 11, no. 1, pp. 49–58, 2022. https://doi.org/10.1541/ieejjia.21002574

[13] H. Zhu and M. Wu, "Direct control of bearingless permanent magnet synchronous motor based on prediction model," *Progress in Electromagnetics Research M*, vol. 101, pp. 127–139, 2021. https://doi.org/10.2528/PIERM20121401

[14] T. Pei, D. Li, J. Liu, J. Li, and W. Kong, "Review of bearingless synchronous motors: Principle and topology," *IEEE Transactions on Transportation Electrification*, vol. 8, no. 3, pp. 3489–3502, Sept. 2022. https://doi.org/10.1109/TTE.2022.3164420

[15] O. Shariati, A. Behnamfar, and B. Potter, "An integrated elitist approach to the design of axial flux permanent magnet synchronous wind generators (AFPMWG)," *Energies*, vol. 15, no. 9, Apr. 2022, Art. no. 3262. https://doi.org/10.3390/en15093262

[16] S. Zhang and F. L. Luo, "Direct control of radial displacement for bearingless permanent-magnet-type synchronous motors," *IEEE Transactions on Industrial Electronics*, vol. 56, no. 2, pp. 542–552, Aug. 2009. https://doi.org/10.1109/TIE.2008.2003219

[17] S. Javadi and M. Mirsalim, "A coreless axial flux permanent magnet generator for automotive applications," *IEEE Transaction on Magnetics*, vol. 44, no. 12, pp. 4591–4598, Dec. 2008. https://doi.org/10.1109/TMAG.2008.2004333

[18] A. A. Idyatulin, S. F. Saparulov, F. N. Saparulov, and S. M. Fatkullin, "Simulation of flank induction rotator of liquid metal," *Russian Electrical Engineering*, vol. 80, no. 7, pp. 392–397, Oct. 2009. https://doi.org/10.3103/S1068371209070086

[19] R. Nauber *et al.*, "Dual-plane flow mapping in a liquid-metal model experiment with a square melt in a traveling magnetic field," *Experiments in Fluids*, vol. 54, Apr. 2013, Art. no. 1502. https://doi.org/10.1007/s00348-013-1502-x

[20] J. Stiller, K. Koal, W. E. Nagel, J. Pal, and A. Cramer, "Liquid metal flows driven by rotating and traveling magnetic fields", *Eur. Phys. Journal Spec. Top.*, vol. 220, no. 1, Mar. 2013. https://doi.org/10.1140/epjst/e2013-01801-8

[21] S. Denisov, M. E. Mann, and S. Y. Khripchenko, "MHD stirring of liquid metal in cilindrical mould with free surface," *Magnetohydrodynamics*, vol. 33, no. 3, pp. 365–374, 1997. http://mhd.sal.lv/contents/1997/3/MG.33.3.9.R.html

[22] H. Branover *et al.*, "On the potentialities of intensification of electromagnetic stirring of melts", *Magnetohydrodynamics*, vol. 42, pp. 291–298, no. 2–3, Sep. 2006. https://ui.adsabs.harvard.edu/abs/2006MHD....42..291B/abstract

[23] I. Kolesnichenko, A. Pavlinov, and R. Khalilov, "Movement of the solid-liquid interface in gallium alloy under the action of rotating magnetic field," *Magnetohydrodynamics*, vol. 49, no. 1–2, pp. 191–199, 2013. https://doi.org/10.22364/mhd.49.1-2.23

[24] I. Kolesnichenko, A. Pavlinov, E. Golbraikh, P. Frick, A. Kapusta, and B. Mikhailovich, "The study of turbulence in MHD flow generated by rotating and traveling magnetic fields," *Experiments in Fluids*, vol. 56, Apr. 2015, Art. no. 88. https://doi.org/10.1007/s00348-015-1957-z

[25] S. Taniguchi *et al.*, "Electromagnetic stirring of liquid metal by simultaneous imposition of rotating and traveling magnetic fields," *Tetsu-to-Hagane*, vol. 92, no. 6, pp. 364–371, 2006. https://doi.org/10.2355/tetsutohagane1955.92.6_364

[26] B. Mikhailovich, O. Ben-David, and A. Levy, "Liquid metal rotating flow under permanent magnetic system impact", *Magnetohydrodynamics*, vol. 51, no. 1, pp. 171–177, 2015. https://doi.org/10.22364/mhd.51.1.16

[27] P. Dold and K. W. Benz, "Rotating magnetic fields: Fluid flow and crystal growth applications", *Progress in Crystal Growth and Characterization of Materials*, vol. 38, no. 1–4, pp. 39–58, 1999. https://doi.org/10.1016/S0960-8974(99)00007-8

[28] O. Kalender and Y. Ege, "A PIC microcontroller based electromagnetic stirrer," *IEEE Transaction on Magnetics*, vol. 43, no. 9, pp. 3579–3585, Sep. 2007. https://doi.org/10.1109/TMAG.2007.902825

[29] S. Bicakci, "On the Implementation of Fuzzy VMC for an Under Actuated System," *IEEE Access*, vol. 7, pp. 163578–163588, Nov. 2019. https://doi.org/10.1109/ACCESS.2019.2952294

[30] R. Rakoczy, "Mixing energy investigations in a liquid vessel that is mixed by using a rotating magnetic field," *Chemical Engineering and Processing: Process Intensification*, vol. 66, pp. 1–11, Apr. 2013. https://doi.org/10.1016/j.cep.2013.01.012

[31] R. Rakoczy, A. Przybył, M. Kordas, M. Konopacki, R. Drozd and K. Fijałkowski, "The study of influence of a rotating magnetic field on mixing efficiency," *Chemical Engineering and Processing: Process Intensification*, vol. 112, pp. 1–8, Feb. 2017. https://doi.org/10.1016/j.cep.2016.12.001

Hakan Citak received the B.S. and PhD degrees from the Department of Electric Education, Institute of Science, Marmara University, Istanbul, Turkey, in 1995 and 2014, respectively.

He is currently working for the Balikesir Vocational High School, Electric Program, Balikesir University, Balikesir. His research interests are magnetism and power electronics. He holds two patents.
E-mail: hcitak@balikesir.edu.tr

Sabri Bicakci was born in Balikesir, Turkey in 1982. He received the B.S. degree in electronics engineering from the Erciyes University, Kayseri, in 2005, M.S. degree in electrical and electronics engineering from the Balikesir University, Balikesir, in 2009 and the PhD degree in mechanical engineering from Balikesir University, Balikesir, in 2012.

From 2005 to 2015, he was a Research Assistant with Electrical and Electronics Engineering Department, Balikesir University. Since 2015, he has been an Assistant Professor with the Mechatronics Engineering Department, Balikesir University. His research interest includes robotics and control systems.
E-mail: sbicakci@balikesir.edu.tr

Mustafa Coramik received the B.S. degree from the Department of Physics Education and PhD degree from the Department of Physics, Institute of Science, Balikesir University, Balikesir, Turkey, in 2012 and 2018, respectively.

He is currently working for the Necatibey Education Faculty and Physics Education Department, Balikesir University, Balikesir. His research interests are magnetism and power electronics.
E-mail: mustafacoramik@balikesir.edu.tr

Huseyin Gunes was born in Istanbul, Turkey in 1984. He received the B.S. degree in Computer and Instructional Technologies from the Balikesir University, Balikesir, in 2007, M.S. degree in Computer and Instructional Technologies from the Balikesir University, Balikesir, in 2010 and the PhD degree in mechanical engineering from Balikesir University, Balikesir, in 2017.

From 2011 to 2017, he was a Lecturer with Ivrindi Vocational School, Balikesir University. Since 2017, he has been an Assistant Professor with the Mechatronics Engineering Department, Balikesir University. His research interest includes artificial intelligence, algorithms and robotics.
E-mail: hgunes@balikesir.edu.tr

Yavuz Ege received the B.S. and PhD degrees from the Department of Physics, Institute of Science, Balikesir University, Balikesir, Turkey, in 1998 and 2005, respectively.

He is currently working for the Necatibey Education Faculty and Physics Education Department, Balikesir University, Balikesir. His research interests are solid state physics, magnetism, and power electronics. He holds two patents.
E-mail: yege@balikesir.edu.tr